Efficiency of Conscious Access Improves with Coupling of Slow and Fast Neural Oscillations

Chie Nakatani[1,2], Antonino Raffone[3], and Cees van Leeuwen[1,2]

Abstract

■ Global workspace access is considered as a critical factor for the ability to report a visual target. A plausible candidate mechanism for global workspace access is coupling of slow and fast brain activity. We studied coupling in EEG data using cross-frequency phase–amplitude modulation measurement between delta/theta phases and beta/gamma amplitudes from two experimental sessions, held on different days, of a typical attentional blink (AB) task, implying conscious access to targets. As the AB effect improved with practice between sessions, theta–gamma and theta–beta coupling increased generically. Most importantly, practice effects observed in delta–gamma and delta–beta couplings were specific to performance on the AB task. In particular, delta–gamma coupling showed the largest increase in cases of correct target detection in the most challenging AB conditions. All these practice effects were observed in the right temporal region. Given that the delta band is the main frequency of the P3 ERP, which is a marker of global workspace activity for conscious access, and because the gamma band is involved in visual object processing, the current results substantiate the role of phase–amplitude modulation in conscious access to visual target representations. ■

INTRODUCTION

Several models of conscious access agree on the premise that it involves large-scale cooperative and competitive interactions between brain areas, rather than specialized processing within segregated modules (e.g., Dehaene, Changeux, Naccache, Sackur, & Sergent, 2006; Maia & Cleeremans, 2005; Block, 2001; Dehaene, Kerszberg, & Changeux, 1998; Tononi & Edelman, 1998; Baars, 1988). The principles of such a global processing architecture were proposed in the global workspace (GW) theory (Baars, 1988, 2002), from which Dehaene and collaborators subsequently developed their computational framework of the global neuronal workspace model (Gaillard et al., 2009; Dehaene et al., 2006; Dehaene, Sergent, & Changeux, 2003).

GW models are relevant to a set of phenomena in which conscious access to visual information is required for task performance (Dehaene et al., 2003). One of these phenomena, the attentional blink (AB), refers to the failure to report a target presented with a characteristic time lag after another target (e.g., Raymond, Shapiro, & Arnell, 1992). In a typical AB task, visual stimuli are presented rapidly and serially in the center of a display (rapid serial visual presentation [RSVP], such as 20 letters at a rate of 10 items per second). Two of the stimuli are targets (T1 and T2), and the rest are nontargets (or distractors). Both targets have to be reported. Whereas participants typically report T1 with nearly perfect accuracy, successful report of T2 depends on its time lag from T1. When the two targets are sufficiently separated in time (500 msec or more), T2 is detected with normal accuracy. But when T2 is presented closer to T1 (200–500 msec after T1), T2 is likely to be missed. This effect is known as the AB phenomenon. When, however, T2 is presented immediately after T1, despite the even greater temporal proximity T2 is reported with near-normal accuracy. This effect is known as Lag 1 sparing (Potter, Chun, Banks, & Muckenhoupt, 1998).

Regarding the AB, Dehaene et al.'s (2003) model studies have suggested that T2 is not encoded in the GW if the GW is still occupied by processing T1. In this respect, the model is in accordance with a two-stage account of the AB (Chun & Potter, 1995). T2 is processed only at a first parallel (perceptual) stage and therefore does not give rise to the global self-sustained activity pattern of the GW supporting conscious access, thus resulting in the AB. Later experiments, however, have cast doubts on the two-stage models, emphasizing the role of flexible control processes in the AB (e.g., Olivers & Watson, 2006; Di Lollo, Kawahara, Ghorashi, & Enns, 2005).

A more recent GW model, the visual selection and awareness (ViSA) model (Simione et al., 2012) incorporates an interactive gating device between lower perceptual processing modules and higher access control modules. The access control modules consist of GW and visuospatial working memory (VSWM) modules. Ongoing recurrent interactions between the access control and perceptual processing modules consolidate targets in the GW, thence encode and maintain them in VSWM. Presentation of T1 leads to inhibition of the

[1]KU Leuven, [2]RIKEN, Brain Science Institute, [3]Sapienza University of Rome

neural representation of T2 in the GW; however, this inhibition rises slowly to become effective only from about 100 msec after T1 onset, thus allowing Lag 1 sparing. In the most difficult condition, at Lag 3 to note, inhibition has risen to weaken the neural activity for T2 in the GW, which, in combination with masking-related decay of activation for T2 in the perceptual processing modules, leads to failure of consolidation for T2 in the GW, prevented encoding in VSWM, hence to the AB. Meanwhile, this effect is reinforced by slowing down of T1 consolidation because of weak bottom–up and recurrent input as a result of brief presentation and masking at perceptual level, which in turn prolongs the inhibition of the T2 representation in the GW. When T2 arrives later, it is no longer affected by the AB: As a result of the release of T1-related inhibition in the GW, encoding of T1 in VSWM is completed. Release of inhibition in the GW allows T2 to be consolidated and encoded in VSWM, hence to be reported. This mechanism explains that T2 report is fully recovered, for example, at Lag 7.

ViSA, thus, provides a neurodynamical account of a range of access consciousness phenomena, including the AB. Note that, in this account, the speed of consolidation and encoding in VSWM are not fixed but depend adaptively on strength and duration of sensory input and recurrent signaling from the access control system to perceptual processing modules. This adaptive processing has consequences for learning, which the model can easily accommodate: practice could improve the efficiency of conscious access. In particular, in AB conditions, the effect will be that T2 in Lag 3 would more often be detected. One way in which this could be realized is through enhanced coupling among the distributed processes of the GW. The possible role of coupling in conscious report efficiency leads us to propose putative neural correlates of this behavior, which can be studied in EEG. In this study, we reanalyzed our EEG data from two AB task sessions held on different days, using a cross-frequency coupling (CFC) measure based on Canolty's method (Canolty et al., 2006).

Cross-frequency Phase–Amplitude Coupling

In EEG signals, slow activities such as delta (<4 Hz) and theta (4–8 Hz) ranges have been related to conscious access (Zylberberg, Dehaene, Roelfsema, & Sigman, 2011; Gaillard et al., 2009; Baars & Franklin, 2003). Moreover, these slow oscillations are dynamically entrained across distributed brain regions by both external sensory input and internal cognitive events (Lakatos et al., 2005, 2009; Schroeder & Lakatos, 2009a, 2009b). During conscious and cognitive tasks, however, fast activities, such as beta (13–30 Hz) and gamma (>30 Hz) bands are also prominent. For example, a large-scale network of activity in the beta and gamma bands has been reported as highly relevant to the AB task (Kranczioch, Debener, Maye, & Engel, 2007; Nakatani, Ito, Nikolaev, Gong, & van Leeuwen, 2005; Gross et al., 2004). Gamma-band activity, in particular lower-gamma (30–50 Hz), has been related to distributed processing of object information, its maintenance and conscious processing (e.g., Wyart & Tallon-Baudry, 2008; Gruber & Muller, 2005; Kaiser & Lutzenberger, 2003; Engel & Singer, 2001; Tallon-Baudry, Bertrand, & Fischer, 2001; Tallon-Baudry, Bertrand, Peronnet, & Pernier, 1998; Tallon-Baudry, Bertrand, Delpuech, & Pernier, 1996). Given the wide frequency range of relevance, coupling between different frequencies, CFC measure is desirable to estimate coupling between the access control and perceptual processing activities.

Recently, several authors have called attention to the functional relevance of CFC between phase and amplitude in cognitive tasks (Canolty et al., 2006, 2010; Lakatos, Karmos, Mehta, Ulbert, & Schroeder, 2008; Demiralp et al., 2007; Lakatos et al., 2005). For example, Canolty et al. (2006) reported coupling between theta band (4–8 Hz) phase and high-gamma band (80–150 Hz) amplitude in electrocorticogram (ECoG) in various cognitive tasks. We may thus observe coupling with slow oscillations of fast oscillatory activities that have been implicated in conscious access by theoretical (Dehaene & Changeux, 2005; Dehaene et al., 2003; Raffone & Wolters, 2001) and empirical studies (Kranczioch et al., 2007; Nakatani et al., 2005; Gross et al., 2004), in particular, between delta/theta and beta/gamma bands.

Scope of the Current Study and Hypothesis

The majority of previous cognitive neuroscience studies on the AB has been focused on the relationship between a transient neural activity (e.g., T1-evoked P3 and T2-evoked N2) and a specific function (e.g., post-T1 inhibition and attentional enhancement of T2; e.g., Nakatani, Bijal, & van Leeuwen, 2012; Chennu, Craston, Wyble, & Bowman, 2009; Sessa, Luria, Verleger, & Dell'Acqua, 2007; Slagter et al., 2007; Kranczioch, Debener, & Engel, 2003; Vogel, Luck, & Shapiro, 1998). Note that the ViSA model also incorporates a mechanism of post-T1 inhibition. The role of such transient mechanisms was analyzed based on ERP methods in Nakatani et al. (2012) and is not considered here.

Here we reanalyzed our EEG data from that study, using a CFC measure based on Canolty's method (Canolty et al., 2006). We should note that a variety of CFC measures has been proposed (Jensen & Colgin, 2007, for a review). Comparisons between various CFC measures have also been reported (e.g., Jirsa & Müller, 2013; Tort, Komorowski, Eichenbaum, & Kopell, 2010; Penny, Duzel, Miller, & Ojemann, 2008). There are basically two methods for computing CFC measures in which, respectively, either instantaneous samples are taken across multiple trials or multiple cycles of activity from single trials are used. The first method produces event time-locked/exogenous measures, as it is computed from multiple trials that are

aligned from the onset of an event (e.g., a stimulus presentation). The second method produces measures that include, besides these signals, spontaneous/endogenous CFC as well.

On the basis of the ViSA model, we predict that the coupling between the phase of access control-related delta/theta oscillatory activity and the amplitude of beta/gamma oscillations encoding perceptual contents for conscious access will increase between sessions of the AB task. In principle, in the current study, we may expect increases in coupling strength to occur either in endogenous or exogenous signals. We, therefore, chose a measure from the second type, namely, the cross-frequency phase–amplitude modulation index (MI; Canolty et al., 2006). The MI is one of the most popular CFC measures. This measure, in combination with EEG frequencies of interest and task in the current study, imposes a limitation: Because the measure requires multiple phase cycles for computation, transient CFC cannot be estimated (further details on this limitation will be discussed in Methods: EEG Recording and Processing).

METHODS

We used the EEG data set from Nakatani et al. (2012), who studied practice effects on AB and ERPs. Therefore, participants, stimuli, task, and data acquisition procedures are the same as those previously reported.

Participants

Thirteen university students (2 men and 11 women, 18–28 years, 20.85 years on average) from Tokyo and its immediate surroundings participated in the experiment. All were right-handed and had normal or corrected-to-normal vision. Participants received a remuneration of ¥1000 per hour. The research ethics committee of RIKEN had approved the experiment.

Stimuli

Stimuli were uppercase letters and digits, excluding G, I, K, X, 0 (zero), and 1 (one). Each stimulus fitted within an area of 1.36° × 1.36° of visual angle. The average luminance value was 11.10 cd/m^2. Seventeen to 20 of the stimuli were shown in RSVP in each trial; SOA was 100 msec and ISI was 80 msec, that is, each stimulus was presented for 20 msec and was followed by a 80-msec blank screen. One of the stimuli was shown in blue as T1. Participants judged if T1 was a letter or a digit; letters or digits occurred in 50/50% of the trials. T1 was presented either at the fifth or eighth position within the RSVP. The rest of the stimuli were letters presented in white color (background color was always gray). T2 was a letter "O," which was present or absent half of the times. When present, T2 occurred as either the first, third, or seventh stimulus after T1 (Lag 1, Lag 3, and Lag 7 trials).

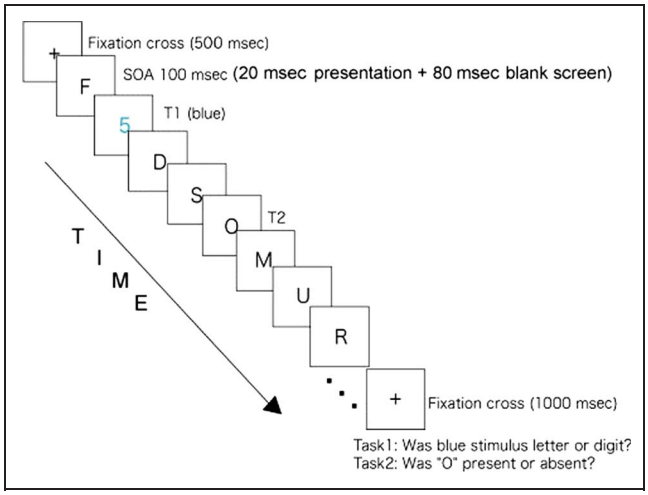

Figure 1. Illustration of experimental task.

At least three distractors, that is, nontarget white letters, followed T2 in the RSVP. Next, a fixation cross was presented for 1000 msec. Participants fixated the cross while waiting for the first response panel. Immediately afterward, the first response panel appeared, prompting participants to identify the category of T1 (letter or digit). This was followed immediately with a second response panel, prompting them to report the presence or absence of T2. Participants had been instructed to make the best guess when they were not sure about their perception. Figure 1 shows the sequence of events in a trial.

Equipment and Procedure

For stimulus presentation, we used a CRT display (Trinitron MultiScan G520, SONY, Tokyo, Japan). Presentation was synchronized with the display refresh rate (100 Hz). The display was placed at eye height, at a distance of 105 cm from the viewer. Participants were seated comfortably in a chair with armrests. Responses were made by pressing the right or left button in a button box with their right middle or index finger—the category of T1 was reported first (letter–right button, digit–left button), then the presence/absence of T2 was reported (present–right button, absent–left button). The button box (Etalcia tenkey box, Elecom, Osaka, Japan) was placed next to their arm rest, in immediate reach of the participant. The experiment took place in a sound-attenuated chamber with dim ceiling lights.

The experiment consisted of two experimental sessions, which were held on two different days (in average 5.69 days apart). On both days, participants completed one experimental session, which consisted of two dual task blocks (T1 and T2 reports were required) and two single task blocks (in which T2 had the same frequency of occurrence as in the dual task block, but only T2 report was required). The blocks alternated in a counterbalanced

order. Each block had 288 trials and consisted of 144 T2 present trials (48 trials × 3 lags) and 144 T2 absent trials in random order. In total, each participant completed 576 dual-task and 576 single-task trials. Before the first experimental session, instruction and 16 practice trials were given. Afterward, the electrodes were attached, and EEG was recorded while participants performed in the experiment. The experiment took about 2.5 hr per session including instruction and EEG preparation time.

EEG Recording and Processing

The experimental tasks were programmed using a software package (SuperLab Pro version 4.0, Cedrus Corporation, San Pedro, CA) running on a Windows XP PC. EEG was recorded with a commercial EEG recording system (EEG1100, Nihon Kohden, Tokyo, Japan) using a cap with 19 tin electrodes (ElectroCap, Electro-Cap International, Inc., Eaton, OH), which were placed according to the international 10–20 system. The ground electrode was placed at the midsagittal line between Fz and Cz. Reference electrodes were placed on left and right ear lobes, which were digitally linked. EOG electrodes were attached at right and left temples for horizontal EOG and at above and below of the left eye for vertical EOG. Data were digitized at 500 Hz (0.1–100 Hz analogue bandwidth). To remove artifacts, the InfoMax algorithm (Makeig, Bell, Jung, & Sejnowski, 1996) was applied to the EEG signals taking the 19 electrodes as factors. Independent components that showed high correlation with vertical or horizontal EOGs and those that showed the profile of a muscular artifact were excluded from EEG signal reconstruction.

Artifact-removed EEG signals from 0.5 to 44 Hz were analyzed; frequencies higher than 44 Hz was not analyzed because of weak signal strength relative to AC (which centered at 50 Hz) and EMG-related noise. The EEG signals were binned to 11 frequency bands of equal, 4-Hz bandwidth (except for the lowest bin, which is 0.5–4.0 Hz). Choice of proportional-to-frequency instead of equal-width binning did not alter the results. The Hilbert transform was applied to the bands to compute instantaneous phase and amplitude. Following Canolty's procedure (Canolty et al., 2006), the MI was computed between delta (0.5–4.0 Hz) phase and amplitude of the higher frequencies. The procedure was repeated for between theta (4.0–8.0) phase and amplitude of the higher frequencies. Complex-valued time series $z(t)$ were computed combing the phase and amplitude as

$$z(t) = A_{\text{high}}(t) * \exp(i * (P_{\text{low}}(t))$$

where $P_{\text{low}}(t)$ is the phase and $A_{\text{high}}(t)$ is the amplitude. Thus, $z(t)$ represents amplitude of the higher frequency at a given low-frequency phase. Over a segment from −500 to +1300 msec from T1 onset, $z(t)$ was averaged (MEAN_{raw}). Nonzero MEAN_{raw} indicates dependence between the phase and amplitude. The dependency was tested for each single trial segment. For statistical evaluation, from each segment, 200 surrogate series were obtained by displacing timing of phase and amplitude data (amplitude time series were cut at an arbitrary time point, then their order was swapped; see Canolty et al., 2006, for more details). For each set of surrogates, the mean ($\text{MEAN}_{\text{surrogate}}$) was computed. The distribution of $\text{MEAN}_{\text{surrogate}}$ was used to test for dependency. The MEAN_{raw} was normalized as

$$\text{MI} = (\text{MEAN}_{\text{RAW}}\mu)/\sigma$$

where μ and σ were the mean and variance, respectively, of $\text{MEAN}_{\text{surrogate}}$. The unit of MI, therefore, is arbitrary.

We checked if the segment length (1800 msec) was sufficient to obtain a reliable coupling measure. For example, a 60-sec segment was used for MI computation in Canolty et al. (2006), and MI ranged from 0 to 10, approximately. The variance of the measure would increase as the segment length (i.e., the number of cycles for MI computation) decreases. In the current study, the segment length (−500 to 1300 msec from T1 in RSVP period) was decided to compute a MI in a single-trial RSVP period. The length holds about 11 theta or 4 delta cycles. For theta-phase pairs, the MI ranged, over electrodes and conditions, from 0 to 10 approximately. The range did not change when a 2800-msec segment, which includes the 1800-msec RSVP period and following fixation period of 1000 msec, was used. Moreover, the scalp distribution and differences between conditions were very similar for the 1800- and 2800-msec segments. For delta-phase pairs, the MI of the 1800-msec segment ranged from 0 to 15, whereas that for the 2800-msec segments ranged from 0 to 10. On the other hand, scalp distribution and differences between conditions were very similar between the two lengths. The results suggest that the segment length increased variance of the measure in delta pairs but did not affect the scalp pattern. In the current study, MI was compared within the same frequency pairs. Thus, we concluded that MI computed from the RSVP segment alone was sufficient for the aim of the current study.

The single trial MIs were averaged within test participants for six trial categories, based on three T1–T2 lags and two T2 results (hit or miss). The mean MI of four 4-Hz bins in beta band (12–16, 16–20, 20–24, and 24–28 Hz) and the other four bins in gamma band (28–32, 32–36, 36–40, 40–44) were averaged to compact results.

RESULTS

Behavioral Results

Details of the behavioral results were published elsewhere (Nakatani et al., 2012). Here, we reproduce only the main results; T2 hit rate was highest in the Lag 7

condition, followed by the Lag 1 condition (i.e., the Lag 1 sparing effect), and lowest in the Lag 3 condition (i.e., the AB effect). The occurrence of AB and Lag 1 sparing effects reproduces the typical behavioral pattern of this task. Across sessions, the T2 hit rates in Lags 1 and 3 conditions were increased with practice (Figure 2). Analyses using signal detection theory (Macmillan & Creelman, 2005) showed that practice effects were not because of a shift in decision bias but because of increased sensitivity. Therefore, the practice effect on T2 detection implies that practice enhances the efficiency of conscious target detection.

EEG Results

Overview of MI Scalp Distribution in Seven Frequency Pairs

Scalp distribution of the phase–amplitude MI in the delta–theta, delta–alpha, delta–beta, delta–gamma, theta–alpha, theta–beta, and theta–gamma are shown in Figure 3. Note that the alpha band (8–12 Hz) contains the main frequency of RSVP (10 Hz). For the sake of overview, the average over the two sessions is presented in Figure 3A. A normalized MI is the distance from the center of bootstrapped MI values following the normal distribution in a complex plane. Thus, we used the probability density function of the normal distribution to indicate a nonzero threshold value for normalized MI. Interelectrode dependence for 19 electrodes was corrected using Bonferroni's method. The corrected nonzero threshold value was 3.28 for $p < .01$, which was exceeded in many electrodes. The scalp distribution of the value differs from one frequency pair to another; the delta–theta pair showed high modulation in midline; the delta–alpha and theta–alpha pairs showed strong modulation in posterior electrodes, which may relate to the RSVP stimulation; the delta–beta and theta–beta pairs showed widely distributed modulation and was slightly weighing on the posterior region; in delta–gamma and theta–gamma pairs, the modulation was also widely distributed and was slightly lower for the midline-parietal region. The results showed that the phase–amplitude relation was not random, not only in the RSVP related but also in other frequency pairs.

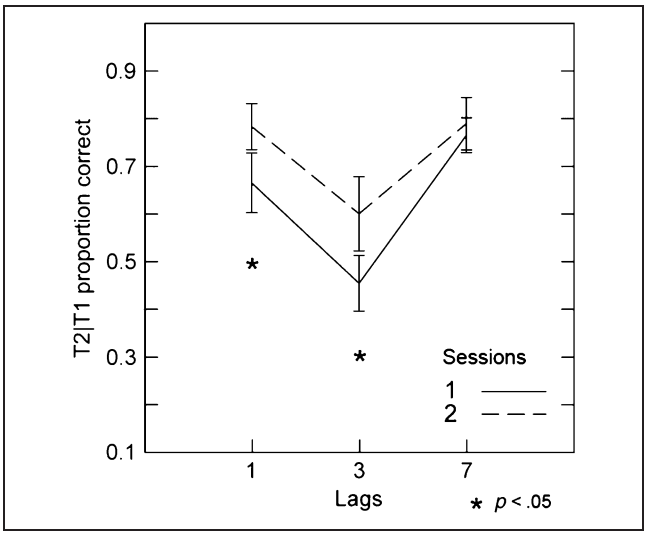

Figure 2. Behavioral measures of T2 report (T2|T1). Proportions of T2 correct report conditional to correct T1 report in three lag conditions (Lags 1, 3, and 7) are plot for each session. Solid and broken lines indicate Sessions 1 and 2, respectively. Asterisks (*) represent $p < .05$, and vertical bars show *SE*. For the complete behavioral results, see Nakatani et al. (2012).

ROIs

As shown in Figure 3B, some regions appeared to show more practice effect than others. Some of them, such as the lateral frontal, parietal, and right temporal regions, were listed as AB-related regions in the EEG/MEG and fMRI literature (e.g., Choi, Chang, Shibata, Sasaki, & Watanabe, 2012; Sergent, Baillet, & Dehaene, 2005; Gross et al., 2004; Marois, Yi, & Chun, 2004; Marois, Chun, & Gore, 2000). We defined our ROIs in accordance with one of the strategies for avoiding circular analysis: "Independent split-data analysis" (Kriegeskorte, Simmons, Bellgowan, & Baker, 2009; see also Kriegeskorte, Lindquist, Nichols, Poldrack, & Vul, 2010). The regions were determined by using the trials that did not include T2, that is, T2 absent trial data. The 19 electrodes were clustered into seven regions: prefrontal (Fp1 and Fp2), frontal (Fz, F3, F4, F7, and F8), central (Cz, C3, and C4), parietal (Pz, P3, and P4), occipital (O1 and O2), right temporal (T4 and T6), and left temporal (T3 and T5). MI values of the correct rejection trials were averaged over the electrodes in each region. To the clustered values, a 2 (Sessions) × 7 (Regions) model was fit in each frequency pair. MANOVA was applied, using the Pillai test, to take into account covariance among the regions. The results showed an interaction between Sessions and Regions in the theta–alpha and theta–gamma pairs: $F(6, 7) = 5.08$, $p = .025$ and $F(6, 7) = 3.68$, $p = .056$, respectively. Paired t tests between the sessions showed that only the right temporal region showed an effect of the sessions: $t(12) = 2.67$, $p = .020$ in theta–alpha and $t(12) = 2.81$, $p = .016$ in theta–gamma pairs. This region was reported as an AB-relevant region in previous EEG/MEG studies (Shapiro, Johnston, Vogels, Zaman, & Roberts, 2007; Gross et al., 2004). Taken together, we considered right temporal as the ROI for the practice effect. Thus, statistical tests for the practice effects in the T2 present trials were conducted only on the right temoral region.

Practice Effects in MI

In the T2 present trials, the MI of the right temporal region were averaged over electrodes (T4 and T6) in each frequency pair. To these averages, a 2 (Sessions) × 3 (Lags) × 2 (T2 hit vs. miss) MANOVA was applied. For

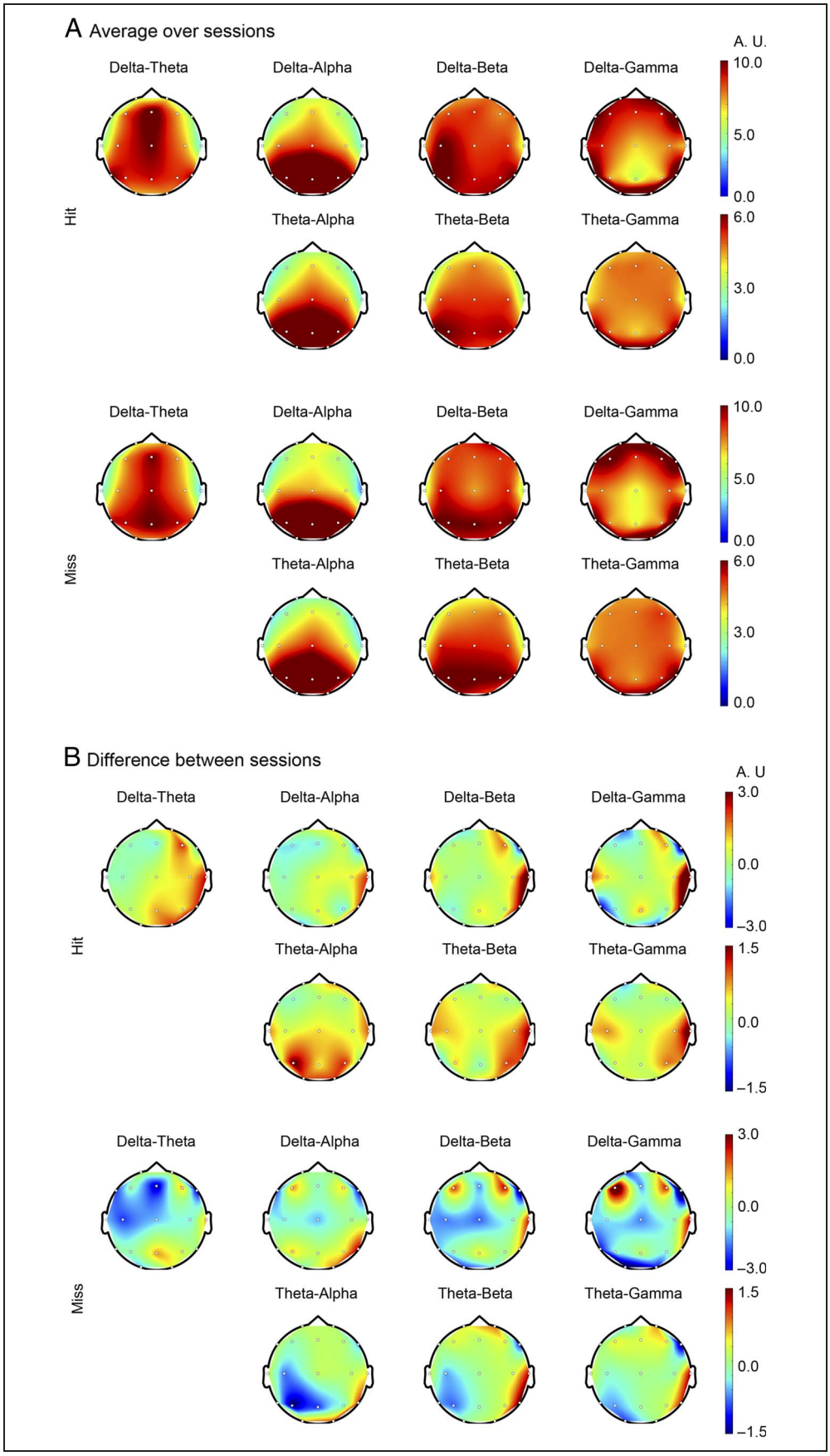

Figure 3. Cross-frequency phase–amplitude MI. (A) Average between sessions for T2 hit and miss trials in the Lag 3 condition. (B) Difference in MI between sessions: $MI_{Session\ 2\ -\ Session\ 1}$. Scalp distribution patterns in other lag conditions were similar to this one. The unit of MI is arbitrary (A.U.).

Table 1. Summary of Practice Effects

	Sessions	*Lags*	*Hit/Miss*	*Sessions × Lags*	*Sessions × Hit/Miss*	*Lags × Hit/Miss*	*Sessions × Lags × Hit/Miss*
Delta–Theta							
Delta–Alpha	*	***					
Delta–Beta				**			*
Delta–Gamma	*			*		**	**
Theta-Alpha	**						
Theta–Beta	**	**					
Theta–Gamma	**						

Results of MANOVA/Pillai's test on the Sessions × Lags × T2 Hit versus Miss model are shown for all frequency pairs. Only effects with $p < .05$ were discussed in the main text.

*$p < .1$.

**$p < .05$.

***$p < .01$.

the theta–alpha, theta–beta, and theta–gamma pairs, a main effect of Sessions was observed: $F(1, 12) = 6.68$, $p = .024$, $F(1, 12) = 8.02$, $p = .015$, and $F(1, 12) = 7.95$, $p = .015$. However, neither the interaction between Sessions and Lags nor the Sessions and T2 hit versus miss were significant. The results are summarized in Table 1. They suggest a nonspecific practice effect, that is, theta phase modulation to the alpha/beta/gamma amplitude increased regardless of the lags and T2 results.

An interaction between sessions and lags was observed in the delta–beta pair; practice increased phase modulation more in the Lags 3 and 7 conditions than the Lag 1 condition (Figure 4A): $F(2, 11) = 5.03$, $p = .028$ for the Sessions × Lags interaction. In the delta–gamma pairs, a three-way interaction (Sessions × Lags × T2 hit vs. miss) was observed, $F(2, 11) = 5.60$, $p = .021$. A breakdown model (2 Sessions × 3 Lags) was fit for the T2 hit and miss trials, separately. In the T2 hit trials, the largest increase appeared in the Lag 3 condition (Figure 4B): $F(2, 11) = 7.29$, $p = .010$ for the Sessions × Lags interaction. In the T2 miss trials, the largest increase appeared in the Lag 7 condition, but the Sessions × Lags interaction was not significant, $F(2, 11) = 2.86$, $p = .100$. In the Lag 7 condition, in particular of the second session, the number of T2 miss trials was smallest among all conditions, so the result in this condition is far less reliable than the other ones.

Effect of Lags and T2 Hit versus Miss

In the delta–alpha pair, the lags showed a main effect; the larger the lags, the higher the MI became: $F(2, 11) = 11.68$, $p = .002$. The theta–beta pair showed the opposite effect; the larger the lags, the lower the MI became: $F(2, 11) = 6.59$, $p = .013$.

None of the pairs showed a main effect of the T2 hit versus miss, whereas this factor showed interactions with

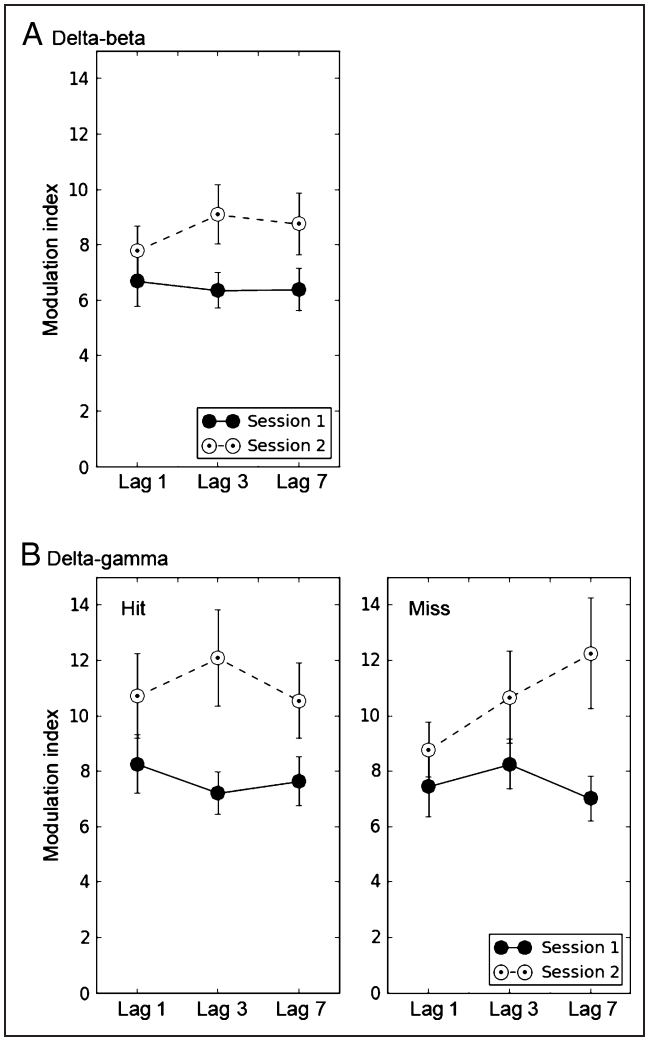

Figure 4. AB task-specific practice effects delta–beta and delta–gamma coupling. (A) The Sessions × Lags interaction in the delta–beta pair. Sessions 1 and 2 are shown in solid and broken lines. Vertical lines represent standard error. (B) The Sessions × Lags × T2 hit versus miss interaction in the delta–gamma pair.

Lags (and Sessions) in the delta–gamma pair, as described. There was also a two-way (Lags × T2 hit vs. miss) interaction, $F(2, 11) = 4.35$, $p = .040$. In the T2 hits, MI was the highest in the Lag 3 conditions, whereas in the misses, it was highest in the Lag 7 conditions, in accordance with the pattern seen in the three-way interaction.

Practice Effects in Target-evoked Responses

Because MI was computed over an 1800-msec RSVP segment, the measure includes both target-evoked and nonevoked phase–amplitude coupling. Some of the target-evoked coupling could, in principle, be a by-product of target-evoked responses; for example, if either the evoked phase reset or amplification increases with practice, the MI would also be increased regardless of ongoing coupling. We therefore checked for practice effects in target-evoked phase consistency and amplitude using the measures phase-locking factor (PLF) and averaged amplitude over single trials (Tallon-Baudry, Kreiter, & Bertrand, 1999; Tallon-Baudry et al., 1998).

In the delta phase, PLF peaked around 300 msec after T1 and T2 (Figure A1). Thus, PLF values between 250 and 350 msec after each target were averaged. In parallel with the MI analysis, PFLs of T4 and T6 electrodes were averaged and submitted to a 2 (Sessions) × 3 (Lags) × 2 (T2 hit vs. miss) MANOVA. An interaction between Sessions and T2 hit versus miss was observed in the post-T1 and post-T2 periods; the corresponding statistics are $F(1, 12) = 9.51$, $p = .009$, and $F(1, 12) = 6.06$, $p = .030$, respectively. However, PLF increased with sessions not in the T2 hit, but in the T2 miss trials. The effect, therefore, was opposite in direction to the MI results.

In the theta phase, PLF values between 150 and 250 msec after each target were averaged, because PLF peaked earlier in the theta than in the delta phase. The 2 × 3 × 2 MANOVA was applied. An interaction between Sessions and T2 hit versus miss was observed: $F(1, 12) = 6.34$, $p = .027$ and $F(1, 12) = 5.49$, $p = .037$ for the post-T1 and post-T2 periods, respectively. Similarly to the delta band, PLF increased with sessions not in the T2 hit, but in the miss trials. This, again, is opposite in direction to the MI results.

Amplitudes during single trial RSVP periods were converted to t values before averaging over trials. The transformation scaled the amplitude, that is, reduced individual differences, thus increased the chance to detect event time-locked changes in the group analysis. In the beta and gamma range, no sizable target time-locked activity was observed. In the alpha band, the amplitude started to increase around 500 msec from T1 onset in all lag conditions. The amplitude between 500 and 1300 msec, which is the end of RSVP, was averaged; next the 2 × 3 × 2 MANOVA was applied. An interaction between Sessions and T2 hit versus miss was observed, $F(1, 12) = 5.74$, $p = .034$. The interaction indicates that alpha power in the T2 miss trials is increased with practice but decreased in the T2 hit trials.

The results indicate that the practice effect in MI in the theta–alpha pair may, at least in part, be explained by the practice effect in alpha power. Target-evoked responses, however, do not account for the practice effects in the MI between delta/theta phase and beta/gamma amplitude, which we will discuss.

DISCUSSION

We studied the effect of practice on conscious target detection and its neural correlates in EEG cross frequency coupling (CFC) in the AB task. Practice enhances the efficiency of second target detection in this task. As we described in the Introduction, the ViSA model (Simione et al., 2012) led us to propose that this improved efficiency is the result of enhanced coupling between the access control and perceptual processing modules.

Practice was found to enhance the coupling between phase of slow and amplitude of fast oscillations in EEG activity. The slow oscillations may be associated with conscious access/control-related operations and the fast ones with encoding and maintaining perceptual contents; according to ViSA model, all these processes are crucial in this task. Enhanced performance on the AB task with practice may therefore be an effect of improved coordination of these processes, reflected in the increased oscillation coupling strength.

General Practice Effects as Reflected in the Cross-frequency Phase–Amplitude MI

Couplings involving different frequency pairs were related to different aspects of practice. The increase in theta–beta/gamma coupling strength with practice did not depend on T1–T2 lags and occurred equally for both T2 hits and misses. In other words, it is a nonspecific practice effect. Theta phase is considered as the carrier for information encoding and read-out, which are the two most fundamental functions of neural information processing and conscious access (Lisman, Talamini, & Raffone, 2005; Jensen, Idiart, & Lisman, 1996; Lisman & Idiart, 1995). Beta and gamma activities are generically observed during human cognitive activity (Buzsáki, 2006; Lopes da Silva, 1991; Gray, König, Engel, & Singer, 1988). A close relationship between beta and gamma band activities has been observed from the neuroreceptor level to the scalp EEG level; both activities arise from an interplay between pyramidal neurons and inhibitory interneurons, in particular, involving $GABA_A$ receptor action (Haenschel, Baldeweg, Croft, Whittington, & Gruzelier, 2000). At the scalp EEG level, the distributions of the beta and gamma power show similarities across various cognitive tasks (Fitzgibbon, Pope, Mackenzie, Clark, & Willoughby, 2004; Tallon-Baudry et al., 1999). Theta-phase modulation of gamma amplitude has been

reported using ECoG and EEG data (Demiralp et al., 2007; Canolty et al., 2006). These collective empirical findings support the notion that theta-phase modulation of beta/gamma amplitude has general relevance to perceptual and cognitive functions. The current results extend these findings to beta amplitude. More importantly, theta–beta/gamma coupling increased with practice in a non-task-specific manner.

AB Task Parameter-specific Practice Effects as Reflected in MI

In contrast with theta modulation, no main practice effect was found in delta–beta/gamma modulation. Instead, the results were specific to AB conditions. Generally speaking, the practice effect was present in Lags 3 and 7 but absent in the Lag 1 condition. In the delta–beta pair, the practice effect was independent of T2 detection, but in the delta–gamma pair modulation increased with practice in the Lag 3 condition only when T2 was detected. Delta phase has been related to cognitive control over target selection (Lakatos et al., 2005, 2008, 2009; Schroeder & Lakatos, 2009b). Also, delta band activity is the frequency of the P3 ERP component, which has been taken to signal the emergence of GW activity (Slagter et al., 2007; Sergent et al., 2005).

Consistently with GW models (e.g., Dehaene et al., 2003), the practice effect in the delta–gamma coupling, therefore, suggests that the AB effect may be reduced by an improved coordination between access/control in the GW and processing and maintaining target representations. Indeed, according to ViSA, the effect of enhanced coordination in conscious access involves an increase in the rate with which target-related activity accrues in the GW. In the model, this leads to more efficient consolidation and encoding in VSWM, especially in the condition characteristic of the AB.

Regions that Showed Practice Effects in the AB Task

We found the coupling effects between slow and fast oscillatory activities in the right temporal region. Given that GW activity is global, how could such a localization of the practice effect be explained? Previous AB studies analyzing individual frequency bands have shown a global functional network in beta and gamma bands (Kranczioch et al., 2007; Nakatani et al., 2005; Gross et al., 2004). In these studies, the right temporal region has been regarded as one of the "hubs" in beta and gamma band synchrony network activity during an AB task. Moreover, the region is suggested as a hub of gamma band activity for working memory maintenance (Park et al., 2012). Phase modulation at the hub might enable access not only to local but also to distributed object information. If so, the local effect could be the tip of an iceberg of a broader brain network activity, which our current, limited methods have failed to more extensively reveal.

Recently, Choi and colleagues reported a practice effect, not in right temporal, but in dorsolateral pFC (DLPFC; Choi et al., 2012). In their study, participants practiced the AB task with a timing cue for T2. As the training eliminated the behavioral AB effect, the BOLD signal decreased in bilateral DLPFC. The authors concluded that the training increased temporal resolution of T1 and T2 processing. Inspired by the fMRI study, we computed the practice effect in amplitude at the frontal electrodes (F3 and F4). To equate the temporal resolution of our signal with the slow BOLD signal, EEG amplitude was averaged over the RSVP period (−500 to 1300 msec from T1 onset). The average amplitude in each frequency band was tested by a 2 Session × 3 Lag × T2 hit versus miss MANOVA/Pillai test. The main effect of and interactions with the Sessions, however, were not statistically significant in any of the frequency bands. The incongruent results could be because of differences in brain signals (BOLD/fMRI vs. EEG amplitude) and/or because of differences in training (AB task practice with or without a T2 timing cue). Further investigation is needed to be conclusive about the inconsistency between these results. However, we should note that our main measure, MI, was introduced to assess coordination between the access/control and perceptual processing modules, based on the ViSA model. The model lists DLPFC as one of the main loci of the access/control activity. The BOLD result, therefore, might indicate practice effects within the access/control system, whereas the current MI results are related to practice effects in coordination between the access/control and perceptual processing modules.

Possible Relationship to Practice Effects on Post-T1 Processes

Besides coupling, ViSA includes another possible mechanism through which practice may, in principle, enhance T2 detection efficiency: post-T1 inhibition. The current results do not bear directly on the relevance of this mechanism. As we mentioned in Introduction and Methods, our MI measure does not possess sufficient temporal resolution to assess such transient effects. Previous studies aimed at these effects have used the temporal resolution of ERPs (Nakatani et al., 2012; Slagter et al., 2007). Results of the previous studies are not unanimous; for example, practice decreased T1-evoked P3b in one study (Slagter et al., 2007), but not in the other (Nakatani et al., 2012).

In a recent RSVP experiment, Wyart and colleagues (Wyart, de Gardelle, Scholl, & Summerfield, 2012) asked their participants for a categorical decision about an entire stimulus series. Individual items contributed to the decision to a degree corresponding to the delta phase at the moment of item presentation. In their account, post-T1 inhibition occurs because of delta-phase locking

to T1. Given that a delta cycle takes about 500 msec, T1 and T2 in a typical AB condition (e.g., T1–T2 lag is 300 msec) would fall in opposite phases of the cycle. Thus, although the evoked response constitutes a phase optimal for processing T1, T2 automatically falls into the worst phase. This prediction illustrates that it might be productive to consider phase modulation for understanding the Attentional Blink.

Future Perspective

GW models are concerned with the way in which distributed subprocesses give rise to a conscious report of a visual percept. ViSA has inherited this property of GW models, with the implementation of an elaborate control mechanism for conscious access in interaction with perceptual processing units. The current version of ViSA is not yet able to simulate EEG signals, although a development for this is on the way. A future ViSA model that explicitly incorporates CFC could demonstrate its effect on enhanced consolidation and encoding of target information. It should take into account that practice enhances the coupling between phase of slow and amplitude of fast oscillations in EEG, as observed here for the AB. The scope of ViSA, however, extends to VSWM tasks, where the same effects of practice could therefore be expected. We are planning to investigate this issue in further joint experimental and computational modeling studies.

APPENDIX

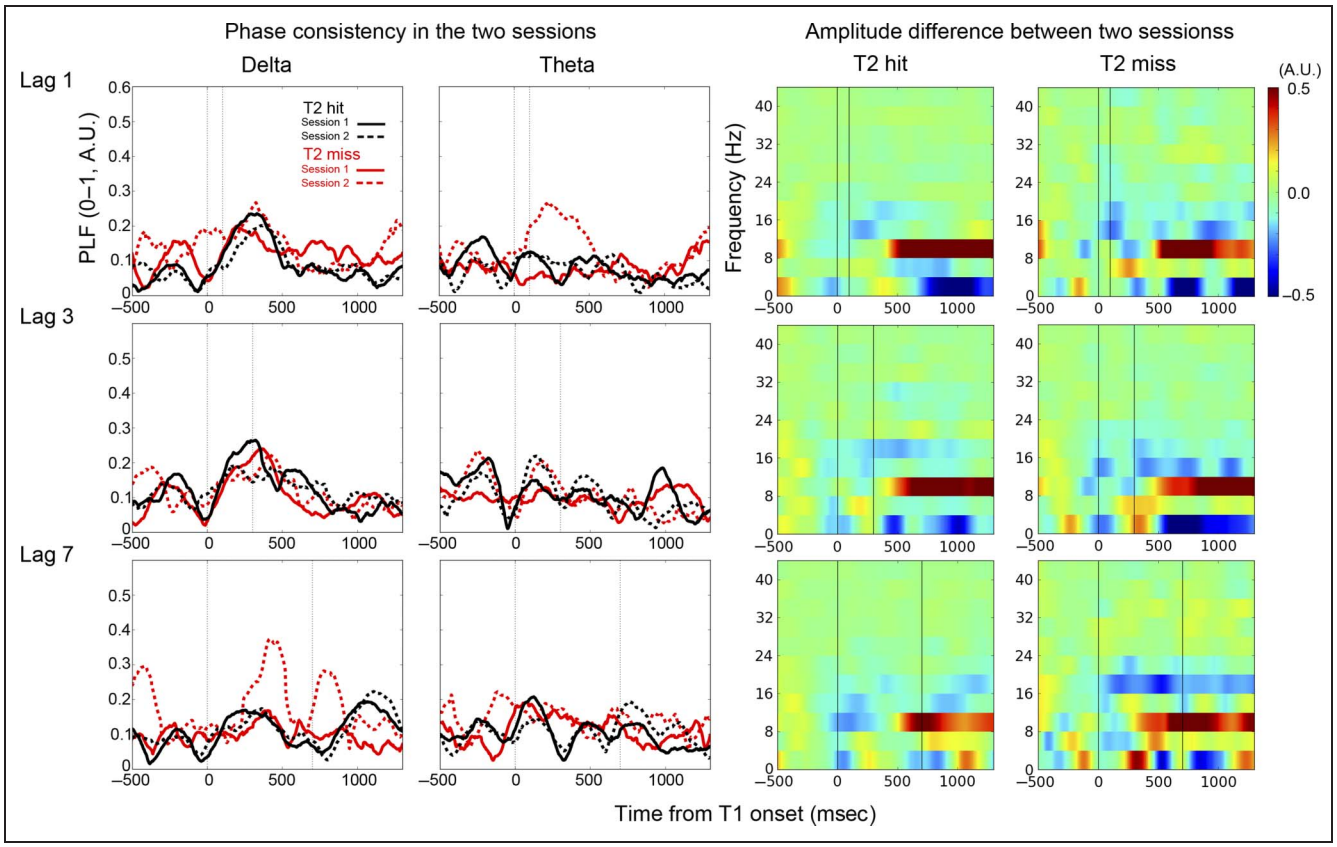

Figure A1. Practice effects in the PLF and average amplitude. Line charts: PLF in Sessions 1 and 2 are shown in solid and broken lines, respectively. T2 hit (black) and miss (red) trials are overlaid. Horizontal axis is time from T1 onset. Vertical lines indicate T1 and T2 onset. Time–frequency plots: Difference in amplitude between two sessions (Session 2 − Session 1) is shown for T1 hit and miss trials, respectively. Before the subtraction, the amplitude was baseline-corrected (baseline period: from −500 to 0 msec) and converted to *t* value for each 4-Hz frequency bin. The alpha, beta, and gamma bands correspond to 4–8, 12–28, and 28–44 Hz, respectively.

Acknowledgments

This study was supported by an Odysseus grant of the Flanders Science Organization FWO, issued to Cees van Leeuwen. We would like to thank anonymous reviewers for their useful comments.

Reprint requests should be sent to Chie Nakatani, Laboratory for Perceptual Dynamics, University of Leuven, Tiensestraat 102, Box 3711, Leuven 3000, Belgium, or via e-mail: chie.nakatani@ppw.kuleuven.be.

REFERENCES

Baars, B. J. (1988). *A cognitive theory of consciousness*. Cambridge: Cambridge University Press.

Baars, B. J. (2002). The conscious access hypothesis: Origins and recent evidence. *Trends in Cognitive Science, 6,* 47–52.

Baars, B. J., & Franklin, S. (2003). How conscious experience and working memory interact. *Trends in Cognitive Science, 7,* 166–172.

Block, N. (2001). Paradox and cross purposes in recent work on consciousness. *Cognition, 79,* 197–219.

Buzsáki, G. (2006). *Rhythms of the brain*. New York: Oxford University Press.

Canolty, R. T., Edwards, E., Dalal, S. S., Soltani, M., Nagarajan, S. S., Kirsch, H. E., et al. (2006). High gamma power is phase-locked to theta oscillations in human neocortex. *Science, 313,* 1626–1628.

Canolty, R. T., Ganguly, K., Kennerley, S. W., Cadieu, C. F., Koepsell, K., Wallis, J. D., et al. (2010). Oscillatory phase coupling coordinates anatomically dispersed functional cell assemblies. *Proceedings of the National Academy of Sciences, U.S.A., 107,* 17356–17361.

Chennu, S., Craston, P., Wyble, B., & Bowman, H. (2009). Attention increases the temporal precision of conscious perception: Verifying the neural-ST model. *PLoS Computational Biology, 5,* e1000576.

Choi, H., Chang, L. H., Shibata, K., Sasaki, Y., & Watanabe, T. (2012). Resetting capacity limitations revealed by long-lasting elimination of attentional blink through training. *Proceedings of the National Academy of Sciences, U.S.A., 109,* 12242–12247.

Chun, M. M., & Potter, M. C. (1995). A two-stage model for multiple target detection in rapid serial visual presentation. *Journal of Experimental Psychology: Human Perception and Performance, 21,* 109–127.

Dehaene, S., & Changeux, J. P. (2005). Ongoing spontaneous activity controls access to consciousness: A neuronal model for inattentional blindness. *PLoS Biology, 3,* e141.

Dehaene, S., Changeux, J. P., Naccache, L., Sackur, J., & Sergent, C. (2006). Conscious, preconscious, and subliminal processing: A testable taxonomy. *Trends in Cognitive Science, 10,* 204–211.

Dehaene, S., Kerszberg, M., & Changeux, J. P. (1998). A neuronal model of a global workspace in effortful cognitive tasks. *Proceedings of the National Academy of Sciences, U.S.A., 95,* 14529–14534.

Dehaene, S., Sergent, C., & Changeux, J. P. (2003). A neuronal network model linking subjective reports and objective physiological data during conscious perception. *Proceedings of the National Academy of Sciences, U.S.A., 100,* 8520–8525.

Demiralp, T., Bayraktaroglu, Z., Lenz, D., Junge, S., Busch, N. A., Maess, B., et al. (2007). Gamma amplitudes are coupled to theta phase in human EEG during visual perception. *International Journal of Psychophysiology, 64,* 24–30.

Di Lollo, V., Kawahara, J., Ghorashi, S. M. S., & Enns, J. T. (2005). The attentional blink: Resource limitation or temporary loss of control? *Psychological Research, 69,* 191–200.

Engel, A. K., & Singer, W. (2001). Temporal binding and the neural correlates of sensory awareness. *Trends in Cognitive Science, 5,* 16–25.

Fitzgibbon, S. P., Pope, K. J., Mackenzie, L., Clark, C. R., & Willoughby, J. O. (2004). Cognitive tasks augment gamma EEG power. *Clinical Neurophysiology, 115,* 1802–1809.

Gaillard, R., Dehaene, S., Adam, C., Clemenceau, S., Hasboun, D., Baulac, M., et al. (2009). Converging intracranial markers of conscious access. *PLoS Biology, 7,* e61.

Gray, C., König, P., Engel, A., & Singer, W. (1988). Oscillatory responses in cat visual cortex exhibit inter-columnar synchronization which reflects global stimulus properties. *Nature, 338,* 334–337.

Gross, J., Schmitz, F., Schnitzler, I., Kessler, K., Shapiro, K., Hommel, B., et al. (2004). Modulation of long-range neural synchrony reflects temporal limitations of visual attention in humans. *Proceedings of the National Academy of Sciences, U.S.A., 101,* 13050–13055.

Gruber, T., & Muller, M. M. (2005). Oscillatory brain activity dissociates between associative stimulus content in a repetition priming task in the human EEG. *Cerebral Cortex, 15,* 109–116.

Haenschel, C., Baldeweg, T., Croft, R. J., Whittington, M., & Gruzelier, J. (2000). Gamma and beta frequency oscillations in response to novel auditory stimuli: A comparison of human electroencephalogram (EEG) data with in vitro models. *Proceedings of the National Academy of Sciences, U.S.A., 97,* 7645–7650.

Jensen, O., & Colgin, L. L. (2007). Cross-frequency coupling between neuronal oscillations. *Trends in Cognitive Sciences, 11,* 267–269.

Jensen, O., Idiart, M. A., & Lisman, J. E. (1996). Physiologically realistic formation of autoassociative memory in networks with theta/gamma oscillations: Role of fast NMDA channels. *Learning & Memory, 3,* 243–256.

Jirsa, V., & Müller, V. (2013). Cross-frequency coupling in real and virtual brain networks. *Frontiers in Computational Neuroscience, 7,* 00078.

Kaiser, J., & Lutzenberger, W. (2003). Induced gamma-band activity and human brain function. *Neuroscientist, 9,* 475–484.

Kranczioch, C., Debener, S., & Engel, A. K. (2003). Event-related potential correlates of the attentional blink phenomenon. *Brain Research, Cognitive Brain Research, 17,* 177–187.

Kranczioch, C., Debener, S., Maye, A., & Engel, A. K. (2007). Temporal dynamics of access to consciousness in the attentional blink. *Neuroimage, 37,* 947–955.

Kriegeskorte, N., Lindquist, M. A., Nichols, T. E., Poldrack, R. A., & Vul, E. (2010). Everything you never wanted to know about circular analysis, but were afraid to ask. *Journal of Cerebral Blood Flow & Metabolism, 30,* 1551–1557.

Kriegeskorte, N., Simmons, W. K., Bellgowan, P. S., & Baker, C. I. (2009). Circular analysis in systems neuroscience: The dangers of double dipping. *Nature Neuroscience, 12,* 535–540.

Lakatos, P., Karmos, G., Mehta, A. D., Ulbert, I., & Schroeder, C. E. (2008). Entrainment of neuronal oscillations as a mechanism of attentional selection. *Science, 320,* 110–113.

Lakatos, P., O'Connell, M. N., Barczak, A., Mills, A., Javitt, D. C., & Schroeder, C. E. (2009). The leading sense: Supramodal control of neurophysiological context by attention. *Neuron, 64,* 419–430.

Lakatos, P., Shah, A. S., Knuth, K. H., Ulbert, I., Karmos, G., & Schroeder, C. E. (2005). An oscillatory hierarchy controlling neuronal excitability and stimulus processing in the auditory cortex. *Journal of Neurophysiology, 94,* 1904–1911.

Lisman, J. E., & Idiart, M. A. (1995). Storage of 7 +/- 2 short-term memories in oscillatory subcycles. *Science, 267,* 1512–1515.
Lisman, J. E., Talamini, L. M., & Raffone, A. (2005). Recall of memory sequences by interaction of the dentate and CA3: A revised model of the phase precession. *Neural Network, 18,* 1191–1201.
Lopes da Silva, F. (1991). Neural mechanisms underlying brain waves: From neural membranes to networks. *Electroencephalography & Clinical Neurophysiology, 79,* 81–89.
Macmillan, N. A., & Creelman, C. D. (2005). *Detection theory: A user's guide* (2nd ed.). London: Erlbaum.
Maia, T. V., & Cleeremans, A. (2005). Consciousness: Converging insights from connectionist modeling and neuroscience. *Trends in Cognitive Science, 9,* 397–404.
Makeig, S., Bell, A., Jung, T., & Sejnowski, T. (1996). *Independent component analysis of electroencephalographic data*. Paper presented at the Advances in Neural Information Processing Systems.
Marois, R., Chun, M. M., & Gore, J. C. (2000). Neural correlates of the attentional blink. *Neuron, 28,* 299–308.
Marois, R., Yi, D. J., & Chun, M. M. (2004). The neural fate of consciously perceived and missed events in the attentional blink. *Neuron, 41,* 465–472.
Nakatani, C., Bijal, S., & van Leeuwen, C. (2012). Curbing the attentional blink: Practice keeps the mind's eye open. *Neurocomputing, 84,* 13–22.
Nakatani, C., Ito, J., Nikolaev, A. R., Gong, P., & van Leeuwen, C. (2005). Phase synchronization analysis of EEG during attentional blink. *Journal of Cognitive Neuroscience, 17,* 1969–1979.
Olivers, C. N., & Watson, D. G. (2006). Input control processes in rapid serial visual presentations: Target selection and distractor inhibition. *Journal of Experimental Psychology: Human Perception and Performance, 32,* 1083–1092.
Park, H., Kang, E., Kang, H., Kim, J. S., Jensen, O., Chung, C. K., et al. (2012). Cross-frequency power correlations reveal the right superior temporal gyrus as a hub region during working memory maintenance. *Brain Connectivity, 1,* 460–472.
Penny, W. D., Duzel, E., Miller, K. J., & Ojemann, J. G. (2008). Testing for nested oscillation. *Journal of Neuroscience Methods, 174,* 50–61.
Potter, M. C., Chun, M. M., Banks, B. S., & Muckenhoupt, M. (1998). Two attentional deficits in serial target search: The visual attentional blink and an amodal task-switch deficit. *Journal of Experimental Psychology: Learning, Memory, and Cognition, 24,* 979–992.
Raffone, A., & Wolters, G. (2001). A cortical mechanism for binding in visual working memory. *Journal of Cognitive Neuroscience, 13,* 766–785.
Raymond, J. E., Shapiro, K. L., & Arnell, K. M. (1992). Temporary suppression of visual processing in an RSVP task: An attentional blink? *Journal of Experimental Psychology: Human Perception and Performance, 18,* 849–860.
Schroeder, C. E., & Lakatos, P. (2009a). The gamma oscillation: Master or slave? *Brain Topography, 22,* 24–26.
Schroeder, C. E., & Lakatos, P. (2009b). Low-frequency neuronal oscillations as instruments of sensory selection. *Trends in Neuroscience, 32,* 9–18.
Sergent, C., Baillet, S., & Dehaene, S. (2005). Timing of the brain events underlying access to consciousness during the attentional blink. *Nature Neuroscience, 8,* 1391–1400.
Sessa, P., Luria, R., Verleger, R., & Dell'Acqua, R. (2007). P3 latency shifts in the attentional blink: Further evidence for second target processing postponement. *Brain Research, 1137,* 131–139.
Shapiro, K. L., Johnston, S. J., Vogels, W., Zaman, A., & Roberts, N. (2007). Increased functional magnetic resonance imaging activity during nonconscious perception in the attentional blink. *NeuroReport, 18,* 341–345.
Simione, L., Raffone, A., Wolters, G., Salmas, P., Nakatani, C., Belardinelli, M. O., et al. (2012). ViSA: A neurodynamic model for visuospatial working memory, attentional blink, and conscious access. *Psychological Review, 119,* 745–769.
Slagter, H. A., Lutz, A., Greischar, L. L., Francis, A. D., Nieuwenhuis, S., Davis, J. M., et al. (2007). Mental training affects distribution of limited brain resources. *PLoS Biology, 5,* e138.
Tallon-Baudry, C., Bertrand, O., Delpuech, C., & Pernier, J. (1996). Stimulus specificity of phase-locked and non-phase-locked 40 Hz visual responses in human. *Journal of Neuroscience, 16,* 4240–4249.
Tallon-Baudry, C., Bertrand, O., & Fischer, C. (2001). Oscillatory synchrony between human extrastriate areas during visual short-term memory maintenance. *Journal of Neuroscience, 21,* RC177.
Tallon-Baudry, C., Bertrand, O., Peronnet, F., & Pernier, J. (1998). Induced gamma-band activity during the delay of a visual short-term memory task in humans. *Journal of Neuroscience, 18,* 4244–4254.
Tallon-Baudry, C., Kreiter, A., & Bertrand, O. (1999). Sustained and transient oscillatory responses in the gamma and beta bands in a visual short-term memory task in humans. *Visual Neuroscience, 16,* 449–459.
Tononi, G., & Edelman, G. M. (1998). Consciousness and complexity. *Science, 282,* 1846–1851.
Tort, A. B., Komorowski, R., Eichenbaum, H., & Kopell, N. (2010). Measuring phase–amplitude coupling between neuronal oscillations of different frequencies. *Journal of Neurophysiology, 104,* 1195–1210.
Vogel, E. K., Luck, S. J., & Shapiro, K. L. (1998). Electrophysiological evidence for a postperceptual locus of suppression during the attentional blink. *Journal of Experimental Psychology: Human Perception and Performance, 24,* 1656–1674.
Wyart, V., de Gardelle, V., Scholl, J., & Summerfield, C. (2012). Rhythmic fluctuations in evidence accumulation during decision making in the human brain. *Neuron, 76,* 847–858.
Wyart, V., & Tallon-Baudry, C. (2008). Neural dissociation between visual awareness and spatial attention. *Journal of Neuroscience, 28,* 2667–2679.
Zylberberg, A., Dehaene, S., Roelfsema, P. R., & Sigman, M. (2011). The human Turing machine: A neural framework for mental programs. *Trends in Cognitive Science, 15,* 293–300.